

miR-497 inhibits tumor growth and migration of osteosarcoma by targeting plexinA4 and CDK6

Z. S. TIAN¹, M. J. YAN¹, S. LI¹, D. CONG¹, Y. Y. WANG^{2,*}, Q. S. ZHU^{1,*}

¹Department of Orthopedics, China-Japan Union Hospital of Jilin University, Changchun 130033, China; ²Department of Spine Surgery, The First Hospital of Jilin University, Changchun 130021, China

*Correspondence: zhuqingsan788@hotmail.com; tedwangyy@hotmail.com

Received January 8, 2020 / Accepted April 8, 2020

MicroRNAs are small non-coding RNAs that regulate gene expression at the post-transcriptional level which have been reported to be involved in the pathogenesis of various cancers. In the present study, we found that miR-497 was downregulated in osteosarcoma tissues. Gain and loss of function studies were carried out to investigate the effect of miR-497 on the growth of osteosarcoma cells. The results indicated that miR-497 inhibited the growth of osteosarcoma cells. Furthermore, bioinformatics analysis predicted plexinA4 and CDK6 as targets of miR-497, which was afterward confirmed by luciferase activity assay and rescue experiments. These findings suggested that miR-497, plexinA4, and CDK6 may serve as novel potential makers for osteosarcoma diagnostics and therapy.

Key words: miR-497, plexinA4, CDK6, osteosarcoma

Osteosarcoma ranks the most common site of bone tumors, and the incidence of osteosarcoma has shown an increased tendency in recent years [1, 2]. The treatments for osteosarcoma include surgery, radiotherapy, chemotherapy, or a combination of modalities. Despite improvements in diagnostic and therapeutic techniques, the 5-year survival rates for patients with osteosarcoma have not increased over the last 20 years [3, 4]. The potentially high incidence of morbidity and low cure rate urgently require novel methods for diagnosing and treatments which rely on biomedical research.

miRNAs are small endogenous (19–24 bp) non-coding RNAs that bind to the partially complementary sites of mRNA and recruit the RNA-induced silencing complex, leading to either inhibition of protein translation or messenger RNA (mRNA) degradation [5, 6]. A variety of studies have reported that miRNAs play critical roles in cell growth, differentiation, apoptosis, and tumorigenesis and they can potentially act as both oncogenes and tumor-suppressor genes in a variety of tumors including osteosarcoma [7–11].

Alteration of the miR-497 level has been consistently found in a variety of other tumor types, including gastric cancer, colorectal cancer, hepatocellular carcinoma, non-small cell lung cancer (NSCLC), melanoma, ovarian cancer (OC), and cervical cancer (CC) [12–16]. For example, miR-497 has been reported to inhibit the growth of gastric cancer cells by

regulating the expression of PDK3 [13]. Moreover, miR-497 was decreased in tumor tissues of patients with lung cancer, and the overexpression of miR-497 could inhibit the growth and invasion of lung cancer cells [14, 15]; furthermore, it has been reported that miR-497 can regulate the expression of CD274 and function as a tumor suppressor in breast cancer [16]. These results suggest that miR-497 has a tumor-suppressive role. miR-497 participates in various tumor processes, thus it could be potentially used as a diagnostic biomarker. However, further investigation is urgently required, such as the specificity for tumors as a diagnostic biomarker, adverse off-target effects, targeting infusion pathway, and so on. There is a long way for application. Only a better understanding of miR-497 and its target genes will allow the successful translation of current research into clinical applications. Therefore, in the present work, we explored the roles of miR-497 in osteosarcoma. We found that miR-497 was downregulated in osteosarcoma and the overexpression of miR-497 could inhibit the growth as well as the migration of osteosarcoma cells via targeting plexinA4 and CDK6.

Patients and methods

Patient specimens. Twelve pairs of osteosarcoma tissues and adjacent normal tissues were obtained from osteosarcoma patients who underwent radical laryngectomy at the

No.2 Hospital of Tianjin Medical University. All samples were snap-frozen with liquid nitrogen and stored at -80°C until processed. All procedures were performed in accordance with the Declaration of Helsinki of the World Medical Association. This study has been approved by the ethics committee of China-Japan Union Hospital of Jilin University.

Cell culture. Human osteosarcoma cell line MG-63 and SAOS-2 cells were purchased from the Cell Bank of the Chinese Academy of Sciences (Shanghai, China), and cultured in DMEM (Hyclone, USA) supplemented with 10% fetal bovine serum (Hyclone, USA) at 37°C in a humidified atmosphere containing 5% CO_2 .

Quantitative real-time PCR. Total RNA was extracted from MG-63 and SAOS-2 cells with Trizol and subsequent ethanol purification for analysis of relative mRNA levels. They were reversely transcribed into cDNA following the manufacturer's instructions (Takara, China). Then qRT-PCR was conducted to detect miR-497 and plexinA4 and CDK6 mRNA using SYBR-green and standard amplification protocols. U6 small nuclear RNA (U6-snRNA) was used as a standard normalization to evaluate the relative expression levels of miR-497. GAPDH mRNA was calculated with the $2^{-\Delta\Delta\text{Ct}}$ method, respectively.

Cell viability and clonability assays. Cell viability was assessed using a Cell Counting Kit-8 (CCK-8, Beyotime, Nantong, China). MG-63 and SAOS-2 cells were seeded in 96-well plates at 3×10^3 cells/ml and incubated for 5 days. After treatment, $10 \mu\text{l}$ CCK-8 solution was added to each well for 1 h at 37°C . Results were measured at 450 nm on a microplate reader (Bio-Rad Laboratories, CA, USA).

For colony formation assay, cells were resuspended in DMEM supplemented with 10% FBS and seeded in 6-well plates at a density of 200 cells/ml. After cultured for 10 days, cells were washed with PBS and fixed in methanol for 15 min. Then the cells were stained with 0.1% crystal violet. Colonies with at least 50 cells were counted and imaged under a microscope (Nikon, Japan).

Flow cytometry. Twenty-four hours after transfection, cells (1×10^6) were harvested and fixed in 75% ice-cold ethanol. Fixed cells were treated with bovine pancreatic containing $2 \mu\text{g/ml}$ DNase (Sigma, CA, USA) for 25 min, and followed by incubating in $20 \mu\text{g/ml}$ propidium iodide (Sigma, CA, USA) for 20 min. Cell cycle analysis was performed on a FACS-Calibur System (BD Biosciences, NJ, USA). The data were analyzed with the Flowjo software and the cell cycle distribution was shown as the percentage of cells in the G0/G1, S, and G2/M populations. Each experiment was carried out in triplicate.

Western blotting. For western blot analysis, cells were lysed in a lysed buffer (Beyotime, China). The protein extracts were separated by sodium dodecyl sulfate (SDS) polyacrylamide gels and transferred to PVDF membranes by voltage gradient transfer. Membranes were blocked with 5% skimmed milk for 60 min and incubated with primary anti-plexinA4 (#3816, 1:500) and anti-CDK6 (#13331, 1:500)

antibodies (Cell Signaling Technology, USA) overnight at 4°C with agitation. Specific secondary antibodies conjugated to horseradish peroxidase (Cell Signaling Technology, USA) were used to incubate the PVDF membranes for 120 min. Then proteins were revealed by chemiluminescence using the ECL kit (Beyotime, Nanjing, China) and imaged with a digital chemiscope (Qinxiang, Shanghai, China).

Oligonucleotides transfection. miR-497 inhibitor and inhibitor control were synthesized by Genechem (Shanghai, China). The overexpression vectors of plexinA4, CDK6, and miR-497 were constructed through cloning the CDS region of plexinA4 as well as CDK6 and the pre-miR-497 sequence into the pcDNA3.1 vector (Promega, WI, USA). All construct sequences were directly confirmed by DNA sequencing. miRNA oligonucleotides were transfected at a concentration of 60 nmol/l using Lipofectamine 2000 (Invitrogen, CA, USA) according to the manufacturer's instructions.

Xenograft model. MG-63 cells were harvested and resuspended in DMEM medium. A total number of $3 \times 10^6/100 \mu\text{l}$ MG-63 cells transfected with miR-497 mimics or mimic control were subcutaneously injected into the posterior flank of the nude mice. Tumor size was measured every 2 days and calculated by the formula: tumor volume = $0.5 \times \text{length} \times \text{width}^2$. On day 17, the mice were sacrificed and the tumors were excised and weighed.

Luciferase activity assay. The wild-type or mutant seed sequence at the predicted 3'UTR of plexinA4 and CDK6 were synthesized and cloned into the pGL3 Luciferase Reporter Vectors (Promega, WI, USA) at the BamHI and NotI sites. The cells were co-transfected with miR-497 mimics or negative control, and vectors carrying the WT or MT 3'UTR. TRL-SV40 plasmid (Promega, WI, USA) was used as a normalizing control. The cells were harvested to detect the activity of luciferase using the Dual-Luciferase Assay (Promega, WI, USA) at 48 h after transfection.

Statistical analysis. Statistical analysis was performed by GraphPad prism (version 7.0, GraphPad Software, Inc., CA, USA). The data were expressed as the mean \pm standard deviation. Differences between the two groups have been analyzed by Student's t-test. Differences for more than 2 groups have been compared by analysis of variance. A p-value <0.05 was set as a significant difference.

Results

Downregulation of miR-497 in osteosarcoma tissues. qRT-PCR was performed to detect the expression levels of miR-497 in osteosarcoma tissues and normal tissues. The results showed that miR-497 was downregulated significantly in the osteosarcoma tissues in comparison with the normal tissues (Figure 1A, $p < 0.01$).

miR-497 overexpression inhibited proliferation and colony formation, meanwhile induced cell cycle arrest in osteosarcoma cell lines. Function studies including proliferation, colony formation, and cell cycle were carried out

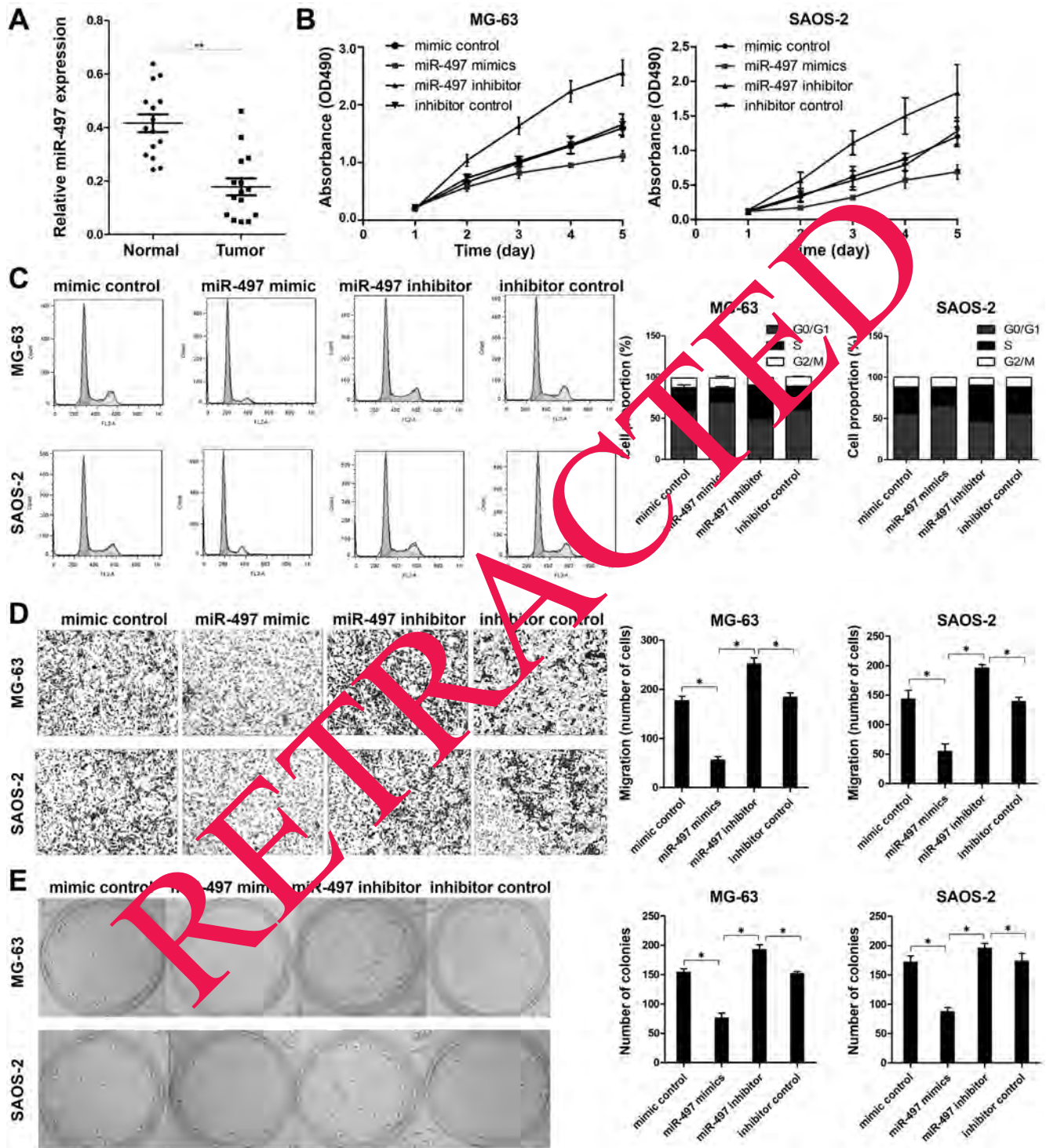


Figure 1. miR-497 inhibited proliferation, colony formation, and induced the G0/G1 cell cycle arrest of osteosarcoma cell lines. A) Quantitative real-time PCR was used to evaluate the expression level of miR-497 in osteosarcoma tissues and adjacent normal tissues. B) MG-63 and SAOS-2 cell viability was examined by MTT assay. C) Cell cycle in each group was detected by flow cytometry. D) Migration abilities of MG-63 and SAOS-2 cells were detected by the transwell experiment. E) Clonability of MG-63 and SAOS-2 cells was detected by colony formation assay. * $p < 0.05$, ** $p < 0.01$

to investigate the effect of miR-497 in osteosarcoma cells. Stable cell lines expressing miR-497 and negative control were established by transfecting with miR-497 mimic and miR-NC. The results revealed that miR-497 overexpression dramatically suppressed the proliferation and colony formation meanwhile induced cell cycle arrest of MG-63 and SAOS-2 cells. On the contrary, miR-497 inhibitor promoted proliferation and colony formation of both MG-63 and SAOS-26 cells, moreover, accelerated the cell cycle progression (Figures 1B–E).

miR-497 directly targeted plexinA4 and CDK6 in osteosarcoma cells. Based on the bioinformatics analysis, a highly-conserved miR-497 targeting sequence was found in the 3'-untranslated regions of the plexinA4 and CDK6 mRNA (Figure 2A). To verify whether miR-497 directly targets plexinA4 or CDK6 in osteosarcoma cell, luciferase activity assays were carried out. As illustrated (Figures 2B, 2C), miR-497 significantly downregulated the luciferase activity in MG-63 and SAOS-2 cells co-transfected with pGL3-3'UTR of both plexinA4 and CDK6 but not with pGL3-3'UTR-mut. Additionally, western blot results indicated that miR-497 significantly decreased the plexinA4 and CDK6 expression at the protein level (Figures 2D–F). On the contrary, the miR-497 inhibitor elevated the expression level of both plexinA4 and CDK6.

PlexinA4 and CDK6 were upregulated in osteosarcoma tissues and were inversely correlated with miR-497 expression. qRT-PCR was performed to detect the expression

levels of plexinA4 and CDK6 in osteosarcoma tissues and normal tissues. The results showed that plexinA4 and CDK6 were upregulated remarkably in the osteosarcoma tissues in comparison with the normal tissues (Figures 3A, 3B, $p < 0.01$). In addition, we observed that the expression level of plexinA4 and CDK6 mRNA expression levels inversely correlated with the expression level of miR-497 in osteosarcoma tissues (Figures 3C, 3D).

The knockdown of plexinA4 and CDK6 attenuated the proliferation and colony formation, meanwhile induced cell cycle arrest in osteosarcoma cell lines. As miR-497 exerted an inhibition effect in the proliferation of MG-63 and SAOS-2 cells, and plexinA4 as well as CDK6 were confirmed to be the targets of miR-497, we next investigated the role of plexinA4 and CDK6 in the regulation of proliferation and cell cycle of MG-63 and SAOS-2 cells. PlexinA4 and CDK6 were knocked down by transfecting with plexinA4-siRNA and CDK6-siRNA respectively. We observed that the knockdown of plexinA4 or CDK6 notably suppressed the proliferation and colony formation meanwhile induced cell cycle arrest of MG-63 and SAOS-2 cells (Figures 4A–D).

The restoration of plexinA4 or CDK6 significantly rescued the miR-497 mediated suppressive effect on cell proliferation. In order to further confirm whether miR-497 inhibits osteosarcoma cell proliferation by directly targeting plexinA4 and CDK6, we carried out a rescue experiment. MG-63 and SAOS-2 cells were co-transfected with the

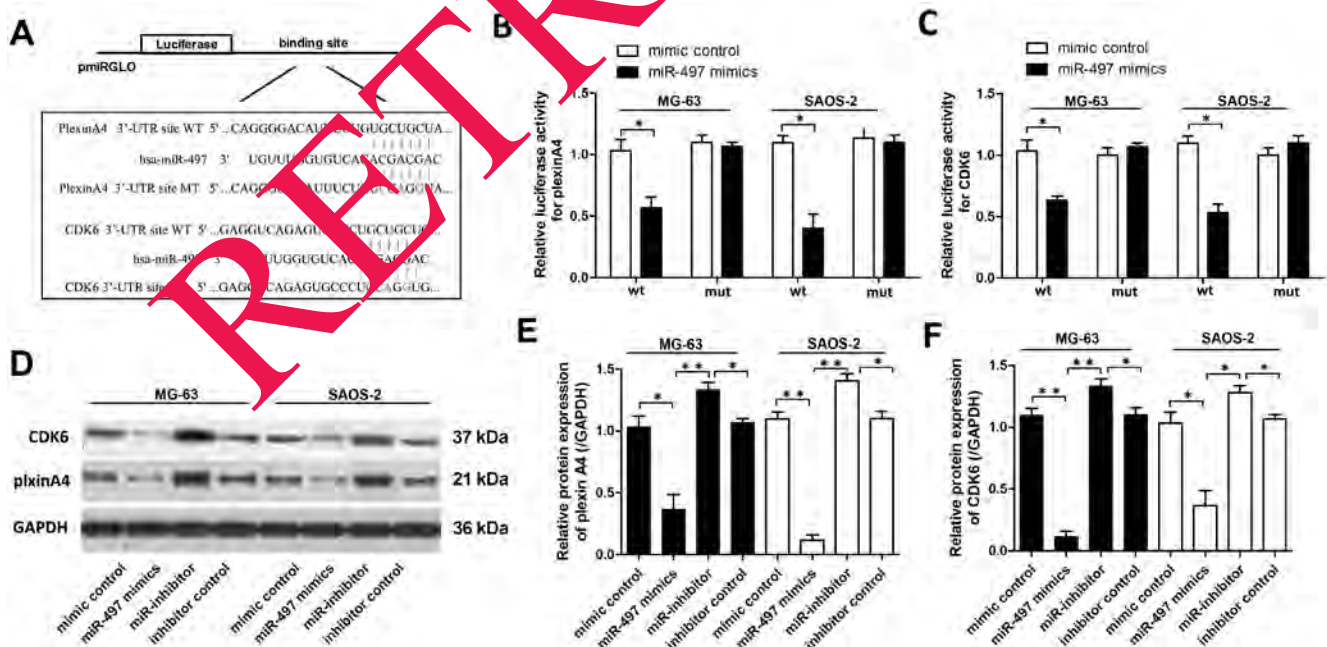


Figure 2. miR-497 directly targeted plexinA4 and CDK6. A) The seed sequences of miR-497 in the WT and MT 3'-UTR of plexinA4 and CDK6 are indicated. B and C) Luciferase activities of reporter vectors in MG-63 and SAOS-2 cells co-transfected with plexinA4-3'UTR-WT as well as CDK6-3'UTR-WT or plexinA4-3'UTR-mut as well as CDK6-3'UTR-mut, along with NC miRNA or miR-497 mimic. D–F) Western blot was used to detect the protein expression level of plexinA4 and CDK6 in MG-63 and SAOS-2 treated with miR-497 mimic or miR-497 inhibitor as well as control. * $p < 0.05$, ** $p < 0.01$

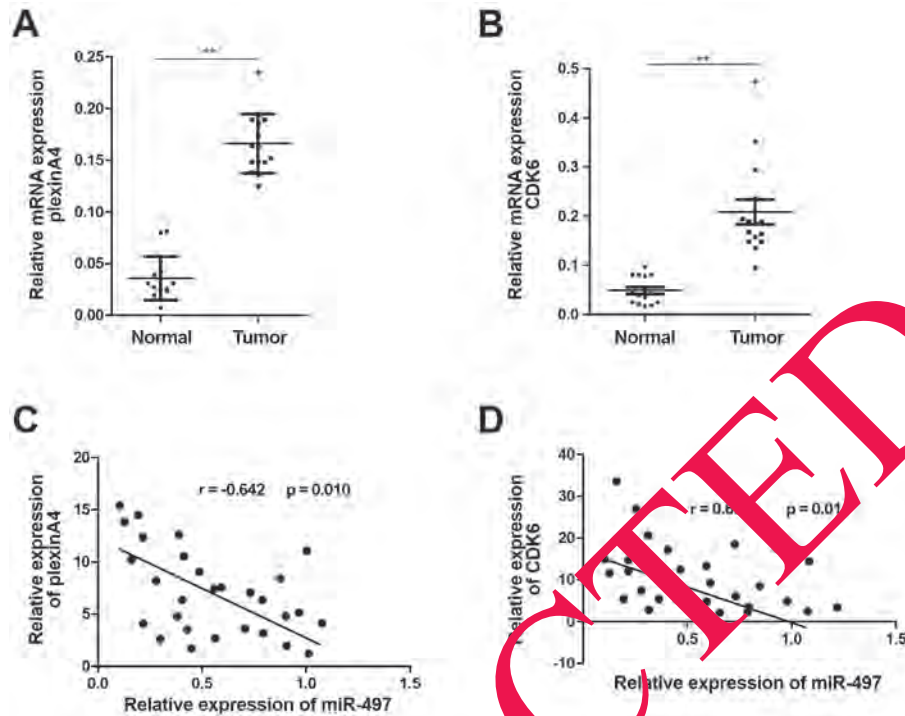


Figure 3. Expression levels of plexinA4 and CDK6 were negatively correlated with the level of miR-497 in osteosarcoma tissue. A and B) qRT-PCR was used to evaluate the expression level of plexinA4 and CDK6 in osteosarcoma tissues and adjacent normal tissues. C) Pearson's correlation scatter plot analysis of the expression levels between miR-497 and plexinA4 protein in osteosarcoma tissues. D) Pearson's correlation scatter plot analysis of the expression levels between miR-497 and CDK6 protein in osteosarcoma tissues. * $p < 0.05$, ** $p < 0.01$

miR-497 mimics and plexinA4 as well as CDK6 overexpression vectors without 3'-UTR. We found that the inhibitory effects of miR-497 on osteosarcoma cell proliferation, invasion, and cell cycle were markedly reversed by plexinA4 and CDK6 overexpression, respectively (Figures 5A–D).

miR-497 suppresses xenograft tumor growth *in vivo*.

To investigate whether miR-497 affects tumor growth *in vivo*, xenograft tumor model was established by subcutaneously injecting MG-63 cells stably overexpressing miR-497 or a blank in the dorsal flank area of nude mice. As expected, compared with the control and blank group, miR-497 overexpression plasmid transfected cells significantly suppressed the tumor growth in nude mice as determined by tumor retarded tumor growth rate (Figure 5E).

Discussion

Increasing evidence has demonstrated that miRNAs regulate the expression of tumor progression related genes, suggesting a new mechanism involved in the initiation and development of various carcinomas. In the present study, we initially demonstrated that the level of miR-497 in osteosarcoma tissues was decreased compared to that in the adjacent normal tissues. Furthermore, gain and loss function experi-

ments revealed that miR-497 inhibited cell proliferation and induced cell cycle arrest in both MG-63 and SAOS-2 cells which suggested that miR-497 indeed plays a critical role in tumorigenesis of osteosarcoma both *in vitro* and *in vivo*.

miRNAs bind primarily to 3'-untranslated regions (3'-UTRs) of target mRNAs leading to repression of translational or mRNA cleavage [10]. More than 1,000 human miRNAs have been identified that regulate approximately 1/3 of the coding genes in the human genome [7, 17, 18]. VEGFA, KSR1, AMOT, ANLN, and HSPA4L have been reported as miR-497 targets in different kinds of tumors. In this work, we used algorithms analysis and plexinA4 as well as CDK6 were selected as the potential target of miR-497.

CDK6 is a member of the CDK family which plays important roles in the major cell-cycle transitions [19, 20]. It governs the cell cycle transitions by initiating the phosphorylation of the RB which leads to the release of E2F transcription factors and subsequently activates the transcription of genes required for S-phase entry. Several studies showed that specific inhibitors of CDK6 have anti-tumor effects in various malignancies making it a widespread attractive molecular biomarker [21, 22].

The plexin family of receptors includes 9 members divided into 4 subfamilies. They are single transmembrane

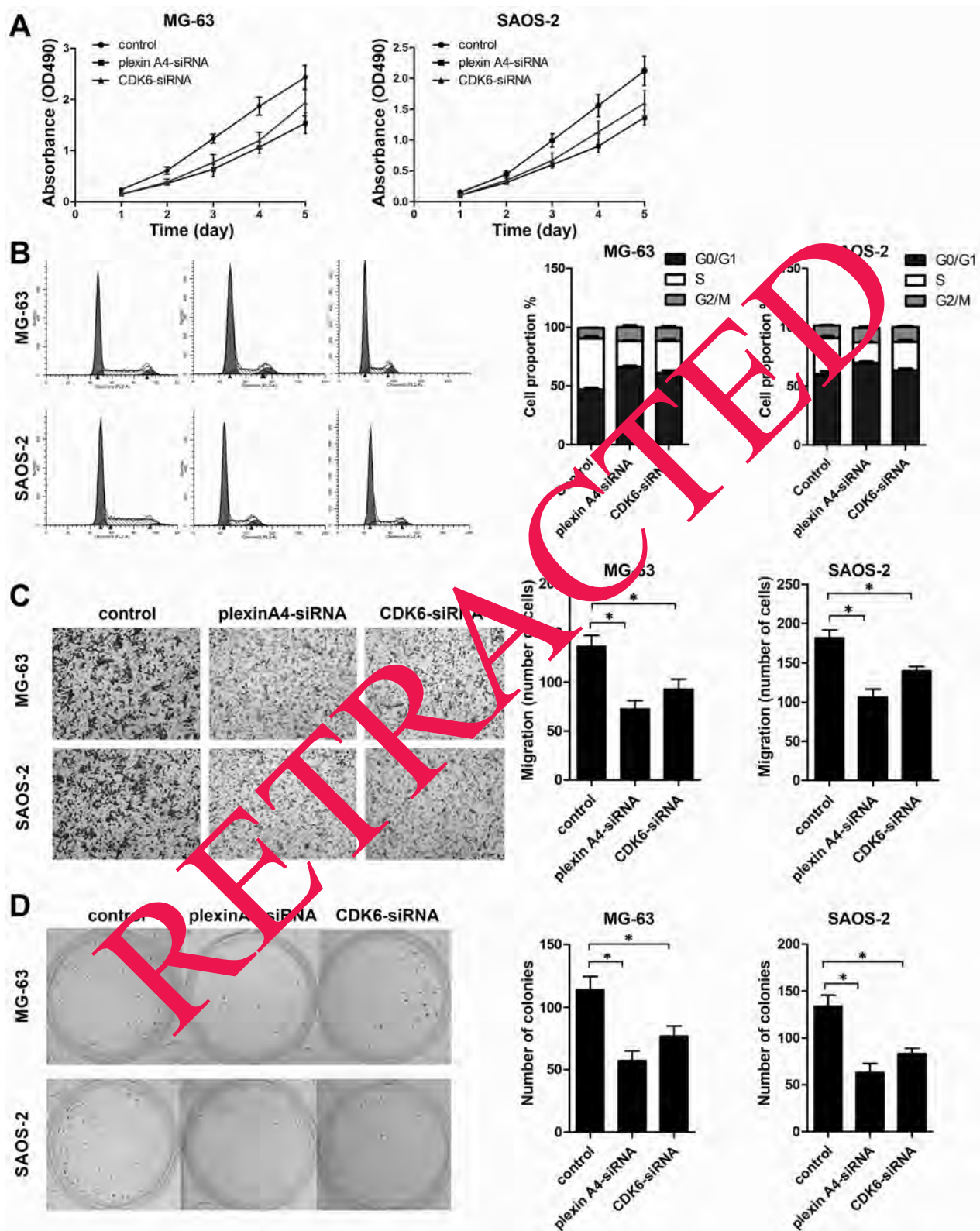


Figure 4. Knockdown of plexinA4 as well as CDK6 inhibited proliferation, colony formation, and induced the G0/G1 cell cycle arrest of osteosarcoma cell lines. A) MG-63 and SAOS-2 cell viability was examined by MTT assay. B) Cell cycle in each group was detected by flow cytometry. C) Migration abilities of MG-63 and SAOS-2 cells were detected by the transwell experiment. D) Clonability of MG-63 and SAOS-2 cells was detected by colony formation assay. * $p < 0.05$, ** $p < 0.01$

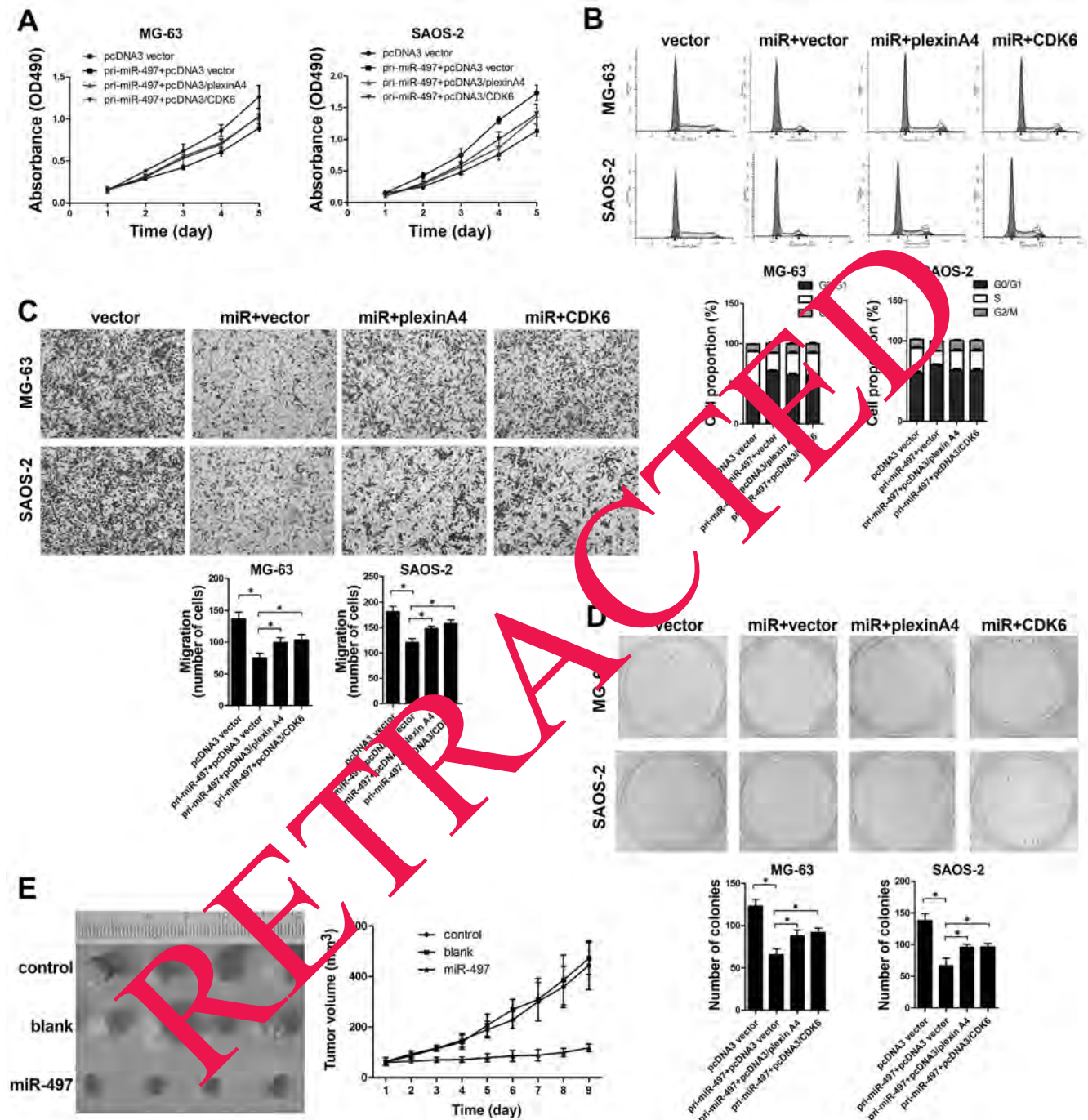


Figure 5. PlexinA4 and CDK6 both reversed the effect of miR-497 on osteosarcoma cell proliferation, clonability, and cell cycle. A) MG-63 and SAOS-2 cell viability was examined by MTT assay. B) Cell cycle in each group was detected by flow cytometry. C) Migration abilities of MG-63 and SAOS-2 cells were detected by the transwell experiment. D) Clonability of MG-63 and SAOS-2 cells was detected by colony formation assay. E) Representative image of tumors formed and the growth curves of tumor volumes. * $p < 0.05$, ** $p < 0.01$

receptors characterized by an intracellular GTPase activating (GAP) domain. The 4 type-A plexins function as direct receptors for class-6 semaphorins that are required simultaneously for the transduction of inhibitory sema3A signals. Kigel et al. found that plexin-A4 combined with FGFR1

and VEGFR-2 tyrosine-kinase receptors and ultimately formed stable compounds that enhanced VEGF-induced VEGFR-2 phosphorylation in endothelial cells as well as bFGF-induced cell proliferation. In addition, they demonstrated that silencing sema6B expression in endothelial

cells and in U87MG cells mimicked the effects of plexinA4 silencing and also inhibited tumor formation from the U87MG cells, suggesting transduction of autocrine sema6B-induced pro-proliferative signals contributed to some of the pro-proliferative effects of plexin-A4 [23].

Interestingly, CDK6 has been confirmed as a target of miR-497 in anaplastic large-cell lymphoma [24], and on the other hand, it has been reported that the levels of CDK6 and miR-497 were negatively correlated in hepatocellular carcinoma [25]; moreover, plexinA4 has been reported as a target of miR-497 in laryngeal squamous cell carcinoma [26]. Therefore, we hypothesized that miR-497 may exert its anti-tumor function in osteosarcoma via targeting plexinA4 and CDK6. In our study, the function study results showed that the knockdown of plexinA4 and CDK6 both inhibited cell proliferation and induced cell cycle arrest, respectively. Moreover, restoration of plexinA4 and CDK6 inhibited miR-497 mediated MG-63 and SAOS-2 cells proliferation inhibition cell cycle arrest. Finally, luciferase assay validated plexinA4 and CDK6 both as direct miR-497 targets.

Our rescue experiments showed that the overexpression of either plexinA4 or CDK6 could only partially blocked the anti-tumor behavior of miR-497. We proposed that this might be because miR-497 has other targets, for example, HMGA2 [27] and Rictor [28], which are oncogenes and which have been proved as the targets of miR-497 in other cancers in previous works. Therefore, in future works, we should also investigate the relationship between miR-497 and those targets in osteosarcoma.

Plexin-A4 is a newly found biomarker representing a target for the development of novel potential anti-angiogenic and anti-tumorigenic drugs. CDK6 has been indicated to be a promising biomarker. We for the first time illuminated the effects of miR-497 in osteosarcoma and the relationship between miR-497 and plexinA4 as well as CDK6. Our findings provide new insight that presents tentative methods for diagnosis, prognosis, and therapy for osteosarcoma.

Acknowledgments: This study was supported by the funds from the Education Department of Jilin Province (NO. JJKH-20190034KJ) and the National Science Foundation of China (NO. 81601957).

References

- [1] MENG Q, TANG B, QIU B. Growth inhibition of Saos-2 osteosarcoma cells by lactucopicrin is mediated via inhibition of cell migration and invasion, sub-G1 cell cycle disruption, apoptosis induction and Raf signalling pathway. *J BUON* 2019; 24: 2136–2140.
- [2] ZHANG Z, PU F, WANG B, WU Q, LIU J et al. Hsa_circ_0000285 functions as a competitive endogenous RNA to promote osteosarcoma progression by sponging hsa-miRNA-599. *Gene Ther* 2020; 27: 186–195. <https://doi.org/10.1038/s41434-019-0112-5>
- [3] RAGHUBIR M, RAHMAN CN, FANG J, MATSUI H, MAHAJAN SS. Osteosarcoma growth suppression by riluzole delivery via iron oxide nanocage in nude mice. *Oncol Rep* 2020; 43: 169–176. <https://doi.org/10.3892/or.2019.7420>
- [4] LI SQ, TU C, WAN L, CHEN RQ, DUAN ZX et al. FGF-induced LHX9 regulates the progression and metastasis of osteosarcoma via FRS2/TGF-beta/beta-catenin pathway. *Cell Div* 2019; 14: 13. <https://doi.org/10.1186/s13008-019-0056-6>
- [5] XIAO F, XIAO S, XUE M. miR-139 Controls Viability Of Ovarian Cancer Cells Through Apoptosis Induction And Exosome Shedding Inhibition By Targeting ATP7A. *Oncotargets Ther* 2019; 12: 1072–10737. <https://doi.org/10.2147/OTT.S221236>
- [6] KUSE N, KAMIO K, AZUMA T, MATSUDA K, INOMATA M et al.: Exosome-derived miR-22 ameliorates pulmonary fibrosis by regulating fibroblast-to-myofibroblast differentiation both in vitro and in vivo. *J Nippon Med Sch* 2019. https://doi.org/10.1272/jnms.JNMS.2020_87-302
- [7] LIU X, CUI M. MiRNA-98-5p inhibits the progression of osteosarcoma by regulating cell cycle via targeting CDC25A expression. *Eur Rev Med Pharmacol Sci* 2019; 23: 9793–9802. https://doi.org/10.26355/eurrev_201911_19542
- [8] HU X, LI L, LU Y, YU X, CHEN H et al.: miRNA-21 inhibition inhibits osteosarcoma cell proliferation by targeting p38EN and regulating the TGF-beta1 signaling pathway. *Oncol Lett* 2018; 16: 4337–4342. <https://doi.org/10.3892/ol.2018.9177>
- [9] GONG N, GONG M. MiRNA-221 from tissue may predict the prognosis of patients with osteosarcoma. *Medicine (Baltimore)* 2018; 97: e11100. <https://doi.org/10.1097/MD.00000000000011100>
- [10] LV S, GUAN M. miRNA-1284, a regulator of HMGB1, inhibits cell proliferation and migration in osteosarcoma. *Biosci Rep* 2018; 38. <https://doi.org/10.1042/BSR20171675>
- [11] HUANG J, LIANG Y, XU M, XIONG J, WANG D et al. MicroRNA-124 acts as a tumor-suppressive miRNA by inhibiting the expression of Snail2 in osteosarcoma. *Oncol Lett* 2018; 15: 4979–4987. <https://doi.org/10.3892/ol.2018.7994>
- [12] CHAE DK, PARK J, CHO M, BAN E, JANG M et al. MiR-195 and miR-497 suppress tumorigenesis in lung cancer by inhibiting SMURF2-induced TGF-beta receptor I ubiquitination. *Mol Oncol* 2019; 13: 2663–2678. <https://doi.org/10.1002/1878-0261.12581>
- [13] FENG L, CHENG K, ZANG R, WANG Q, WANG J. miR-497-5p inhibits gastric cancer cell proliferation and growth through targeting PDK3. *Biosci Rep* 2019; 39. <https://doi.org/10.1042/BSR20190654>
- [14] LI G, WANG K, WANG J, QIN S, SUN X et al. miR-497-5p inhibits tumor cell growth and invasion by targeting SOX5 in non-small-cell lung cancer. *J Cell Biochem* 2019; 120: 10587–10595. <https://doi.org/10.1002/jcb.28345>
- [15] MA W, FENG W, TAN J, XU A, HU Y et al. miR-497 may enhance the sensitivity of non-small cell lung cancer cells to gefitinib through targeting the insulin-like growth factor-1 receptor. *J Thorac Dis* 2018; 10: 5889–5897. <https://doi.org/10.21037/jtd.2018.10.40>

- [16] YANG L, CAI Y, ZHANG D, SUN J, XU C et al. miR-195/miR-497 Regulate CD274 Expression of Immune Regulatory Ligands in Triple-Negative Breast Cancer. *J Breast Cancer* 2018; 21: 371–381. <https://doi.org/10.4048/jbc.2018.21.e60>
- [17] XU YQ, XU Y, WANG SH. Effect of exosome-carried miR-30a on myocardial apoptosis in myocardial ischemia-reperfusion injury rats through regulating autophagy. *Eur Rev Med Pharmacol Sci* 2019; 23: 7066–7072. https://doi.org/10.26355/eurrev_201908_18748
- [18] ZHANG XF, YANG Y, ZHANG J, CAO W. Microvesicle-containing miRNA-153-3p induces the apoptosis of proximal tubular epithelial cells and participates in renal interstitial fibrosis. *Eur Rev Med Pharmacol Sci* 2019; 23: 10065–10071. https://doi.org/10.26355/eurrev_201911_19574
- [19] KUJAN O, HUANG G, RAVINDRAN A, VIJAYAN M AND FARAH CS. CDK4, CDK6, cyclin D1 and Notch1 immunocytochemical expression of oral brush liquid-based cytology for the diagnosis of oral leukoplakia and oral cancer. *J Oral Pathol Med* 2019; 48: 566–573. <https://doi.org/10.1111/jop.12902>
- [20] VALKOV N, KING ME, MOELLER J, LIU H, LI X et al. MicroRNA-1-Mediated Inhibition of Cardiac Fibroblast Proliferation Through Targeting Cyclin D2 and CDK6. *Front Cardiovasc Med* 2019; 6: 65. <https://doi.org/10.3389/fcvm.2019.00065>
- [21] LI Y, LIU J, LIU ZZ, WEI WB. MicroRNA-145 inhibits tumour growth and metastasis in osteosarcoma by targeting cyclin-dependent kinase, CDK6. *Eur Rev Med Pharmacol Sci* 2016; 20: 5117–5125.
- [22] ZHU K, LIU L, ZHANG J, WANG Y, LIANG J et al. MiR-29b suppresses the proliferation and migration of osteosarcoma cells by targeting CDK6. *Protein Cell* 2016; 7: 434–444. <https://doi.org/10.1007/s13238-016-0277-2>
- [23] KIGEL B, RABINOWICZ N, VARSHAVSKY A, KESSLER O, NEUFELD G. Plexin-A4 promotes tumor progression and tumor angiogenesis by enhancement of VEGF and bFGF signaling. *Blood* 2011; 118: 4285–4296. <https://doi.org/10.1182/blood-2011-03-341388>
- [24] HOAREAU-AVEILLA C, QUELEN C, CONGRAS A, CAILLET N, LABOURDETTE D et al.: miR-497 suppresses cycle progression through an axis involving CDK6 in ALK-positive cells. *Haematologica* 2019; 104: 347–359. <https://doi.org/10.3324/haematol.2018.195131>
- [25] FURUTA M, KOZAKI KI, TANIMOTO K, TANAKA S, ARII S et al.: The tumor-suppressive miR-497-195 cluster targets multiple cell-cycle regulators in hepatocellular carcinoma. *PLoS One* 2013; 8: e70155. <http://doi.org/10.1371/journal.pone.0060155>
- [26] NIU JT, LIU SC, HUANG YW, et al. [The effect of miR-497 on laryngeal squamous cell carcinoma invasion through modulating Plexin-A4]. *Zhonghua Er Bi Yan Hou Tou Jing Wai Ke Za Zhi* 2018; 54: 124–130. <https://doi.org/10.3760/cma.j.issn.1673-0860.2018.02.008>
- [27] ZHOU ZG, LI C, DONG Z, WANG YP, DUAN JY et al. MiR-497 inhibits cell proliferation and invasion ability by targeting HMG-A2 in pancreatic ductal adenocarcinoma. *Eur Rev Med Pharmacol Sci* 2020; 24: 122–129. https://doi.org/10.26355/eurrev_202001_19901
- [28] ZHANG M, WU J, ZHANG R, YANG J, ZHANG Q et al. miR-497 inhibits the carcinogenesis of hepatocellular carcinoma by targeting the Rictor/Akt signal pathway. *Int J Clin Exp Pathol* 2019; 12: 1992–2000.